JET-P(95)03

Observations of MHD Activity in JET High Performance Plasmas

M F F Nave[1], B Alper, P Smeulders, S Ali-Arshad, P Lomas, F Marcus, E Monticelli, V Parail, R Sartori, M F Stamp.

JET Joint Undertaking, Abingdon, Oxfordshire, OX14 3EA, UK.
[1] Associação EURATOM/IST, Instituto Superior Técnico, Lisbon, Portugal.

Preprint of a paper to be submitted for publication in the Proceedings of the 1994 International Conference on Plasma Physics, Brazil.

February 1995

ABSTRACT

High performance plasmas were obtained in many JET experiments, both before and after the major shut down of 1992-93. In this paper, a summary is presented, of the MHD activity which , in both the old and the new JET configuration, appears to be most clearly correlated to the collapse of the neutron yield. The paper will discuss aspects of MHD observations in three types of performance limitation; a) slow roll-overs of the neutron rate, which appear to start with the growth of low n modes in the outer 30% of the plasma, b) sawteeth coupled to ELMs, and c) giant ELMs.

1. INTRODUCTION

High performance H-modes have been successfully obtained in several JET experiments. Enhancement factors, $H=\tau_E/\tau_{E(ITER\ 89P)}$, between 2 and 4 have been reached in three types of regimes /1/: Pellet Enhanced Plasma (PEP) H-modes /2/, high β-poloidal H-modes /3/ and hot-ion H- modes /4-6/. In addition, high performance studies in high plasma current discharges, Ip=3-5 MA, have recently been initiated /7/. While the aim of these experiments is to achieve high confinement in a steady-state, the high performance phase is found to be transient, lasting <2 sec. Thus the understanding of the causes of the loss of the high confinement is at present of primarily importance.

Among a varied phenomenology, possibly indicating a variety of causes which may limit high performance, one finds in all types of regimes, cases where the loss of confinement appears to be associated to MHD activity /1/. The most clear cases where MHD activity has a limiting effect, are those where the collapse of the neutron rate occurs following a giant ELM or a large sawtooth crash. In this paper we will discuss aspects of the MHD phenomena which appear to have a limiting effect in hot-ion H-modes, which is the regime where the highest neutron yields have been achieved in JET /6/.

High performance plasmas were obtained both before and after JET's major shut down of 1992-93. During the shut-down, the JET vessel was extensively modified in order to accommodate new installations, which include a pumped divertor, a torus cryopump and new target plates /8/. As a consequence of better designed target plates and better power handling, large Carbon Blooms, which were one of the limitations to high performance in the previous JET configuration /9/, are no longer observed. Without the Carbon Blooms, we are able to study more clearly other underlying causes of the limitation of the high confinement.

From the point of view of MHD observations, there is a marked difference between the observation of edge activity in the old and the "new" JET machine. While the previous JET H-modes were nearly ELM-free, the new ones are more ELMy. This has some advantages, but also some disadvantages. In the new machine configuration, steady-state H-modes in the

presence of small ELMs lasting up to 20s were obtained /10/. In high performance plasmas, on the other hand, a common limitation to achieving high neutron yields are now giant ELMs, which have larger amplitudes and occur more often than what used to be observed.

A detailed analysis of MHD observations in hot-ion H modes up to the JET 1992 shut-down can be found in reference /11/. In the present paper a summary of the MHD activity which appears to be most clearly correlated to the collapse of the neutron yield, both in the old and the new JET configuration is presented. Section II starts with a summary of the observed phenomenology. The following 3 sections, describe observations of low m/n modes (section III), sawteeth combined with ELMs (section IV) and giant ELMs (section V). The ELM section will show data on the giant ELM precursors and ELM global effects which were not discussed in reference /11/.

2. TYPES OF TERMINATION OF HIGH PERFORMANCE

An overview of the JET discharge with the highest neutron yield in a DD plasma is given in fig. 1. This was obtained in a series of hot-ion H mode discharges run in preparation to the JET preliminary tritium experiments of Nov. 1991 /6 /. The time evolution of the D_α emission and temperature signals shown in fig.1, indicate that the high performance phase coincides with a period free of sawteeth and nearly free of ELMs. An early sawtooth,at 12.4s, and the early, small amplitude ELMs, have no large effect on confinement, and do not prevent the development of a high performance regime. The high confinement phase, H>1, lasts ~900ms, and it finishes with a slow roll-over of the plasma stored energy and the neutron rate. This is also the time when the hot-ion H-mode regime is lost as T_i decreases to the same level as T_e. During the phase of termination of high performance, a slow increase in D_α emission and in impurity level is observed. At the end of this phase a sawtooth crash occurs almost simultaneously with a large ELM.

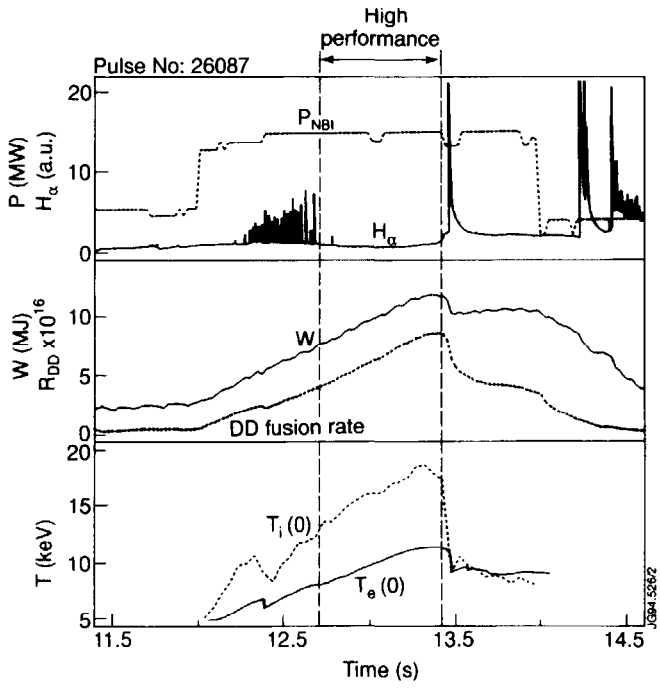

Fig.1 Time evolution of the best D-D discharge. The high performance phase, when H>1, is free of sawteeth and ELMs.

Fig.2 shows the total neutron rate and the CIII line emission for 3 discharges exemplifying different types of termination phases. Case (a) will be referred to as a "slow

termination", since a slow increase in CIII emission is observed coinciding with the collapse of the neutron rate. Cases (b) and (c) show fast increases in CIII emission, which in both cases coincide with a large MHD phenomenon. In case (b) the collapse of the neutron rate coincides with an ELM, while in case (c) it coincides with a sawtooth shortly followed by an ELM. In many discharges, e.g. the best DD discharge shown in fig. 1, we observe a combination of a slow roll-over, as in (a), followed by either a large ELM or a sawtooth combined with an ELM.

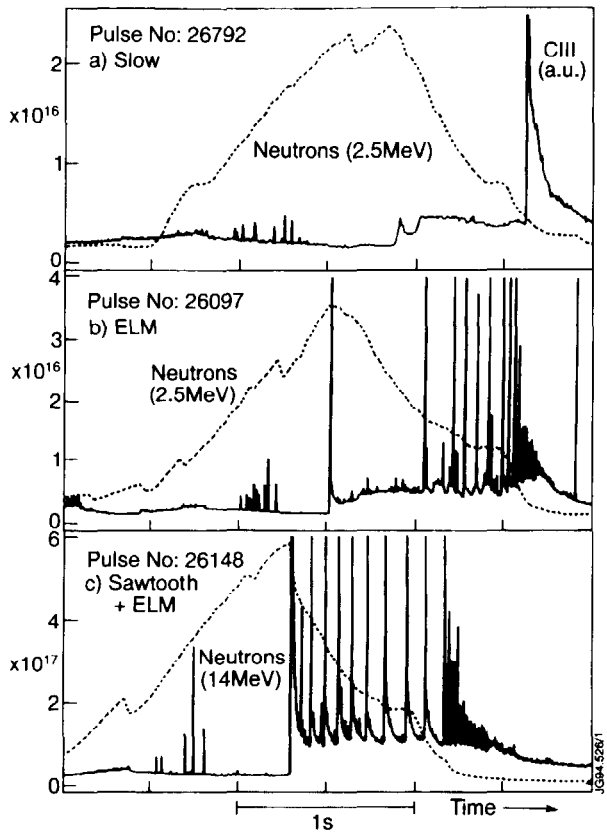

Fig.2 Total neutron rate (broken line) and CIII emission line(solid line) for discharges showing different types of termination of the high performance. (Pulse 26148 is a D-T discharge with 10%T.)

3. OBSERVATIONS OF MHD ACTIVITY DURING THE SLOW TERMINATION

The slow termination starts with a gradual temperature collapse. which is initially observed outside the q=1 region, typically within the outer 30% of the plasma. During this phase, a rich variety of MHD oscillations is observed in all layers of the plasma /11/. In the outer region, where the temperature profile is first affected, coherent oscillations with frequencies of 5-9kHz are observed. These have low toroidal n numbers, in most cases n=1.

Figures 3 and 4 show in detail the slow termination example, case (a), of figure 2. The top traces in figure 3 give the total neutron rate and β_t. The roll-over of the neutron rate occurs when the normalized beta toroidal $\beta_N=\beta_\phi/(I(MA)/a(m)B_\phi(T))$ =1.7 (i.e. at 60% of the Troyon limit). It coincides with a slow collapse of the temperature, which starts in a region outside q=1. Figure 4 shows that, in this case, two types of n=1 activity are observed during the slow collapse. Fishbone oscillations with frequencies around 15kHz (close to the frequency of rotation of the plasma at q=1), and a slower mode with a frequency of 7kHz. The temperature collapse in the outer region of the plasma, and the slow increase in D_α which is a characteristic signature of the termination phase, is well correlated with the growth of the slow n=1 burst.

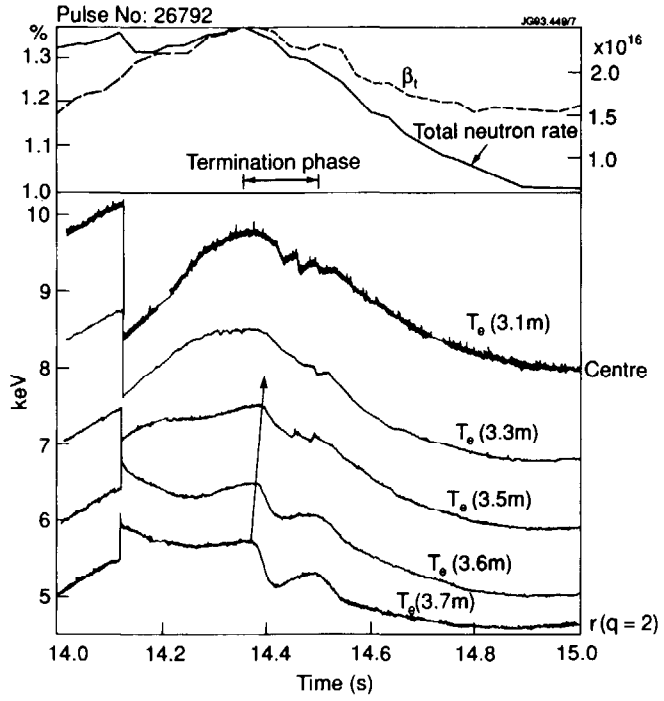

Fig.3 Time evolution of β_t, neutron rate and ECE signals for a slow termination, case (a) of fig. 2. The neutron rate roll-over starts with a temperature collapse, observed first around q=2.

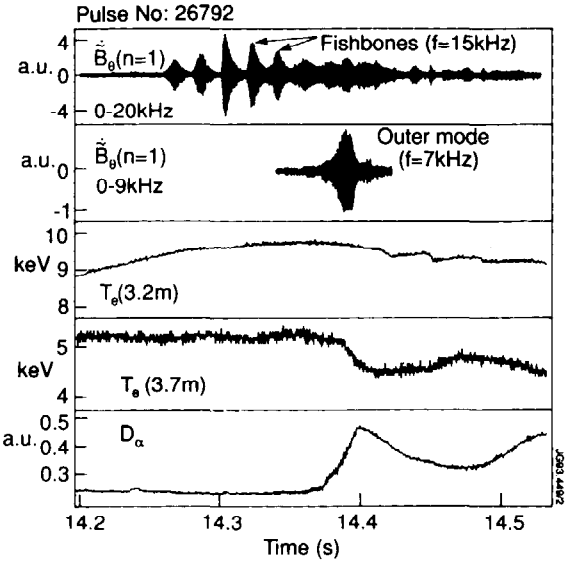

Fig.4 n=1 MHD activity observed during the slow termination phase: a) n=1 signal; b) n=1 signal with central modes filtered out; c) ECE traces; and e) D_α emission. The slow temperature collapse coincides with the growth of the slower, outer, n=1 burst.

The coincidence between the beginning of the slow termination phase and the appearance of n=1 (and sometimes n=2) modes has been observed in many discharges. However the estimated island sizes, in some cases are small, e.g. only a few cms for a m=2, n=1 island in the example above, thus it is difficult to understand how they could have a large effect on confinement /11/. Recent measurements with an infra-red camera show that the slow MHD burst is followed by an increase in the temperature of the target plates. An influx of impurities is observed to follow by a process not yet fully analysed.

4. SAWTOOTH EFFECTS AT THE EDGE

The sawtooth observed in high performance discharges have features which extend beyond the q=1 surface. Those observed at the termination of the high performance are often followed by ELM activity in a few tens of μs. A sawtooth combined with an ELM has been only observed for β_N>1.4.

Fig.5, shows a sawtooth collapse at an intermediate β value, β_N=1.1, observed with a SXR camera at the top of the machine. The several traces show the SXR emission in lines of sight crossing the mid-plane at a position R. The centre of the plasma is at R~3.1 m. The signals from the core of the plasma show the oscillations of an m=1, n=1 precursor. The sawtooth collapse is clearly observed in the central signal. As the m=1, n=1 precursor grows and the central emission collapses, a fast perturbation with a ballooning character is observed to move towards the edge. This causes a transient bulging of the flux surfaces beyond q=1, on the low field side.

The radial extent of the MHD perturbation increases as beta increases. Fig.6 shows the amplitude of the perturbation observed on the low field side for two sawtooth crashes observed in the best DD discharge (shown in fig. 1): a) an early sawtooth, just before the high performance sawtooth-free period, at β_N~0.8; and b) the sawtooth at the termination phase, at β_N ~2.2. For the sawtooth at the termination phase, the perturbation has a finite amplitude at the edge, corresponding to a displacement on the midplane low-field side of ~5 cm. Modelling indicates that the finite MHD amplitude at the plasma boundary could be explained by coupling of the m=1 precursor to higher poloidal harmonics /12/. The perturbation reaches the edge in 20 μs. An ELM follows in <50 μs.

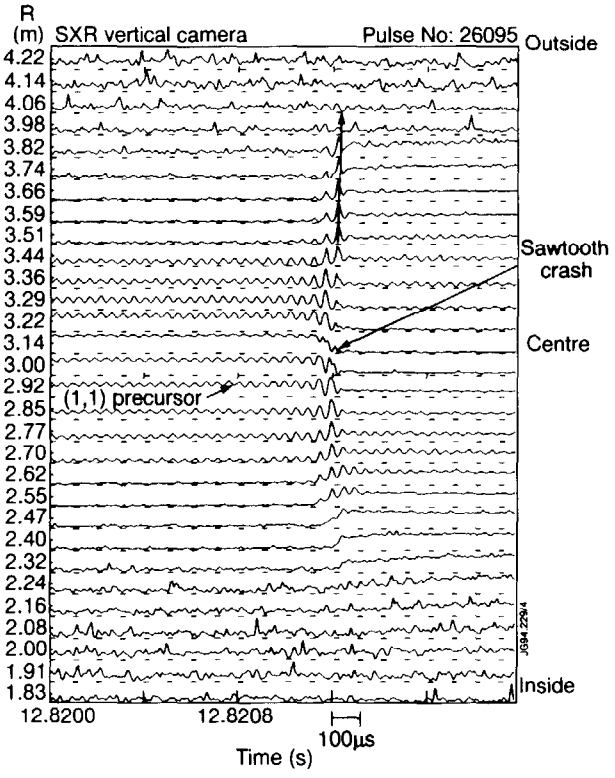

Fig.5 Data from the vertical SXR camera for a sawtooth at an intermediate β value, βN=1.1. A perturbation at the time of the sawtoth collapse extends to large values of R.

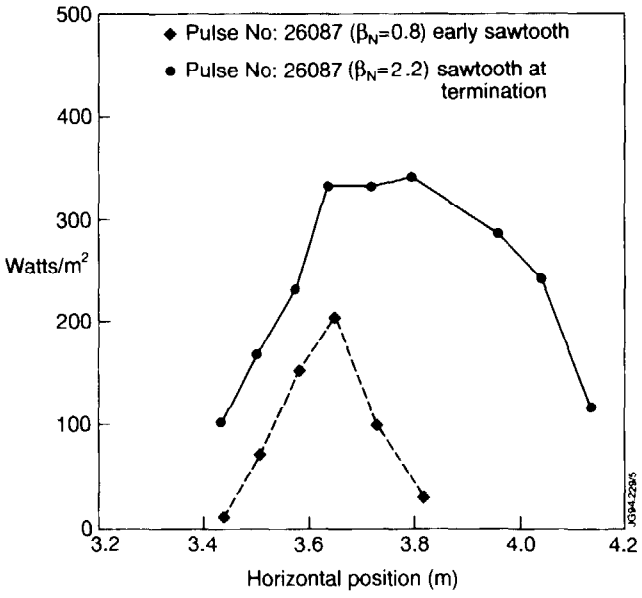

Fig.6 An illustration of how the sawtooth perturbation grows with β. The magnitude of the perturbation in line integrated SXR emission is plotted as a function of radius on the midplane, low field side.

5. GIANT ELMS

The term giant ELM is applied at JET to bursts of H_α emission with amplitudes above 10^{15} ph/s/sr/cm^2. The H_α burst consists of a fast spike lasting ~1 ms and a slow decay phase which for giant ELMs lasts from a few tens to a few hundred ms. Although the name "edge localised mode" is appropriate to describe the MHD precursors to the ELM, the effect that the giant ELMs have on the plasma profiles is certainly not restricted to the edge. This is illustrated in figure 7, where one can see that the larger the ELM, the larger is the effect on the temperature and the further in this effect is observed.

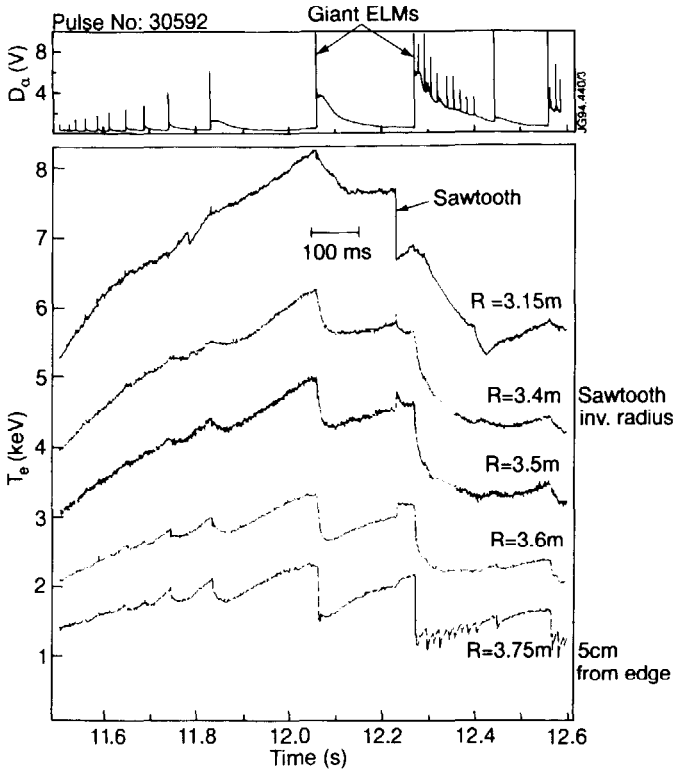

Fig.7 D_α signal and ECE signals at different radii showing that giant ELMs affect the whole temperature profile.

The giant ELMs observed at the termination of the high performance in JET are similar to DIII-D type I ELMs /13/. Like in DIII-D these ELMs are observed late in the H-mode when the edge pressure seems close to the ideal ballooning limit /7/. Since the highest fusion performance is obtained during an ELM-free period, a lot of effort has been put in trying to extend the ELM-free period. It became quite clear that the ELM frequency depends on the plasma shape, and it has been found that an effective way to increase the duration of the ELM-free period is to increase the plasma triangularity and magnetic shear /7/.

Below, two aspects of the observations of giant ELMs will be described: a) the associated MHD oscillations, and b) global effects observed with the SXR cameras.

5a) Precursors and observed mode structure

The L to H transition is normally attributed to a reduction of fluctuations in the plasma. Nevertheless, immediately following the transition, a large variety of high frequency coherent modes, f >30 kHz, and large toroidal mode numbers n=3-12, start to be observed. These high frequency modes grow throughout the H-mode until interrupted by an ELM. Some of these long-lived, high frequency, coherent modes present a sudden growth before the ELM and are know as ELM precursors /14/. In the case of giant ELMs, low frequency precursor oscillations are also observed. These are often much short lived than the high frequency

precursors, being observed in the magnetic pick-up coils only within a few ms of the H_α spike. The giant ELM itself has mainly a low frequency, low n mode structure , as can be seen in fig.8.

Fig.8 shows the observed mode structure for a large ELM which terminates an H-mode. The H_α and magnetic pick-up coil data shown here, have been digitized together allowing a precise timing between the events observed in the two sets of data. A long lived high frequency precursor f ~80 kHz was observed both in magnetic and edge reflectometer signals (see fig.4 in reference /14/). At 0.5 ms before the H_α spike, an n=4 mode with frequency of 15 kHz starts to grow, followed in 0.2 ms by an n=2 mode.

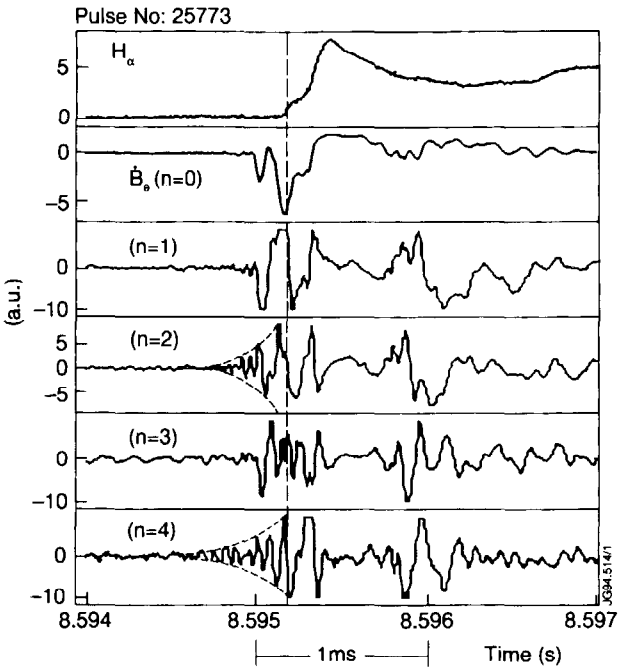

Fig.8 D_α and magnetic pick-up coil signals showing precursors to a giant ELM.

The large amplitude components of the ELM itself are n=0 (>40 Gauss), and n=1 (>15 Gauss). The n=0 component correspond to a movement of the plasma. In the new JET divertor configuration, the plasma is in most cases observed to move inwards and upwards, consistent with a loss of β_p.

Measurements with ECE, SXR and density reflectometry diagnostic systems indicate that both high frequency and low frequency precursors are localized within 5 cm from the edge. (Although their growth may sometimes be triggered by an MHD event in the core, as in the sawtooth/ ELM combination discussed in the previous section.)

5b) Global effects

Although the MHD phenomena starts near the edge, it is quite clear from fig.7, that a giant ELM may provoke a collapse of the temperature in the whole plasma. The JET X-ray diode arrays are particularly suitable to study global ELM effects, as they have the advantage of a high spatial and temporal resolution. Figures 9 and 10, below, show a giant ELM, associated with the termination of high performance, observed with the SXR cameras. For contrast, the figures also show a core MHD phenomena, a fishbone which occured 220ms before the ELM activity.

Figure 9 shows an H_α signal and 4 SXR signals from around the edge, measured with a SXR camera viewing the plasma from the top. In this example, the sampling rate of the SXR data is 10 kHz. The outermost SXR signal shows several spikes corresponding to ELM

activity. Preceding the largest ELM there is an n=1 oscillation with a frequency of 3.4 kHz. Further in, the effect of the ELM is observed, first as a fast collapse of the SXR emission, $\Delta t \sim$ 1 ms, followed by a slower increase of the emission. In order to find out how far in radius those effects are observed a tomography inversion of the SXR /15/data was performed. The temporal resolution is too low to determine the extent of the chaotic zone in great detail, however it does allow the study of the slower peak in the emission that follows the ELM.

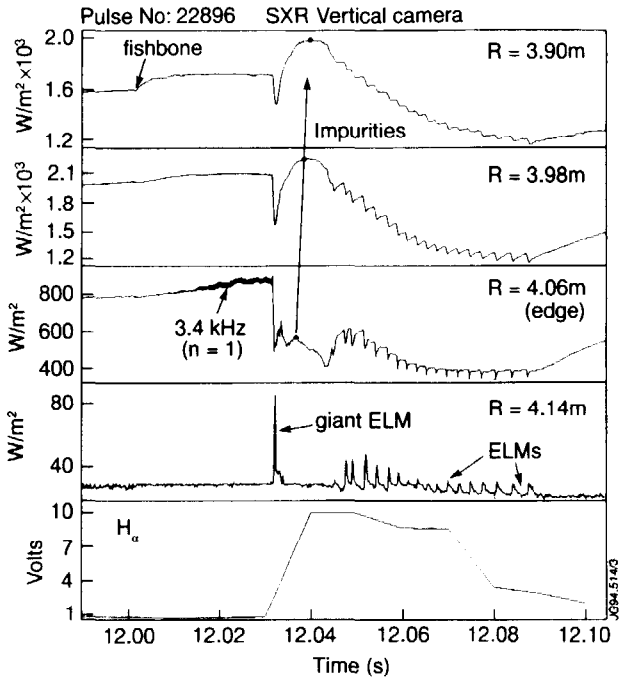

Fig.9 D_α and SXR line integrated signals near the edge showing ELM activity at the termination of a high performance phase.

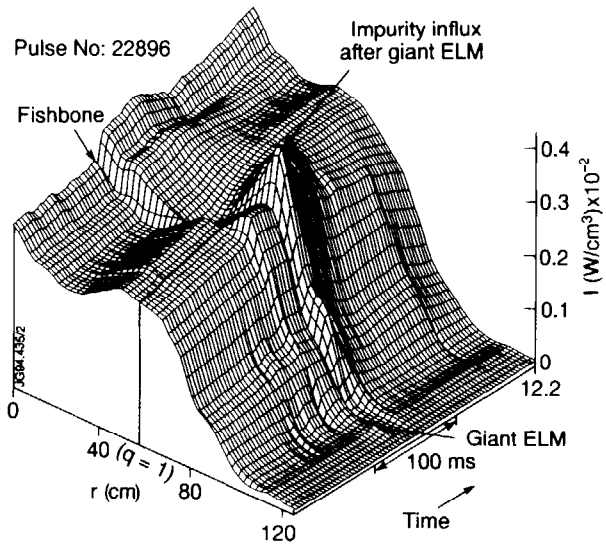

Fig.10 SXR intensity profiles (2-camera tomography). 12ms after the giant ELM, a peak in SXR emission is observed at r(q=1).

Figure 10 shows the temporal evolution of the SXR intensity profiles. The SXR emisson increase which follows the giant ELM is observed up to the q=1 radius. This change in the SXR profiles after the ELM is similar to observations in laser blow-off experiments, where the diffusion of impurities injected at the edge is studied /16/. The time from the observation of the ELM at the edge to the peak at q=1 is 12ms. This is a a very short time, shorter than the time for diffusion of impurities in an H-mode, an possibly 5-10 times shorter than in an L-mode /16/. The figure also shows a fishbone, which is a phenomenon occurring around q=1. Its observed effects are similar to those of sawteeth crashes. Here, since the central SXR profile is hollow, we are able to observe an increase in the central SXR emission. Thus the fishbone, similar to a sawtooth, brings to the core of the plasma impurities which were outside the q=1 region, in an anomalously fast time scale /16/.

6. SUMMARY

Three main types of MHD phenomena are found associated to the termination of high performance in JET experiments: low n number modes in the outer third of the plasma, sawteeth coupled to ELMs, and giant ELMs.

During the phase of termination of the high performance both sawteeth and ELMs lose their local characteristics. The sawtooth, normally thought as a core phenomena, couples to edge activity. Typically, the sawtooth in this phase is followed by an ELM in <50 μs. On the other hand, the large ELMs, although starting with an MHD phenomena close to the edge, are seen to affect the temperature and SXR emission profiles of the whole plasma.

An increase in SXR emission after a giant ELM appears to indicate an impurity influx from the edge to the q=1 radius, in a time shorter than the time for impurity diffusion, which is observed with laser blow-off experiments during L-modes.

A much more subtle type of limitation to high confinement in hot-ion H-modes, known as the "slow termination", appears to start with the growth of low frequency modes in the outer 30% of the plasma. These modes have low toroidal mode numbers n=1-4, the most common observation being that of n=1 modes around the q=2 and q-3 surfaces.

REFERENCES

/1/ JET Team (presented by D. Stork), Plasma Phys. and Contr. Fus. **36**, suppl. 7A (1994) A23

/2/ P. Smeulders et al, "Survey of pellet enhanced performance JET discharges", JET-P(94)07, accepted by Nuc. Fus.

/3/ C. D. Challis et al, Nuclear Fusion **33** (1993) 1097

/4/ Thompson, E, Stork, D., de Esch, H.P.L.and the JET Team, Phys, of Fluids B**5** (1993) 246

/5/ Balet, B. et al. , Nuc.Fus. **33** (1993) 1345/

/6/ JET Team, Nucl. Fus. **32** (1992) 187

/7/ JET Team (presented by P.Lomas), 15th Int. Conf. on Plasma Phys. and Contr.Fus. Research, Seville,Spain (1994), IAEA-CN-60/A-2-I-4

/8/ JET Team (presented by A.Tanga), Plasma Phys. Control Fusion **36** (1994) B39

/9/ D. Stork et al, Proc. 18h EPS Conf. on Contr. Fusion & Plasma Phys., (Berlin) vol. 1 (1991) 357

/10/ JET Team (presented by D.Campbell), 15th Int. Conf. on Plasma Phys. and Contr.Fus. Research, Seville, Spain (1994), IAEA-CN-60/A-4-I-4

/11/ M.F.F.Nave et al., " MHD activity in JET Hot ion H-mode discharges", JET-P(93) 79, accepted by Nuc. Fus.

/12/ B. Alper et al, Procc. 21th EPS Conf. on Contr. Fus. and Plasma Phys., (Montpellier) vol.1, p.202, 1994

/13/ Zhom et al., Proc. 19th EPS Conf. Contr. Fusion & Plasma Phys.,(Innsbruck) vol. I (1992) 243

/14/ Ali-Arshad et al., Proc. 19th EPS Conf. Contr. Fusion & Plasma Phys.,(Innsbruck) vol. I (1992) 227

/15/ R. S. Granetz and P.Smeulders, Nuc. Fus. **28** (1988)462

/16/ D. Pasini et al., Plasma Phys. and Controlled Fusion **34** (1992) 677

ACKNOWLEDGEMENTS

We would like to thank M. Garriba, S. Clement, J. Wesson, R.Gill, R. Giannella and J. Cordey for useful discussions. M.F.F.Nave is gratefull to Fundação de Amparo a Pesquisa do Estado de São Paulo and Fundação Gulbenkian, Lisbon, for the financial support for attendance to this conference.